A Perspective on the Investigation of Spectroscopy and Kinetics of Complex Molecular Systems with Semiclassical Approaches

Riccardo Conte,* Chiara Aieta,* Marco Cazzaniga,* and Michele Ceotto*

Dipartimento di Chimica, Università degli Studi di Milano, via Golgi 19, 20133 Milano (Italy)

E-mail: riccardo.conte1@unimi.it; chiara.aieta@unimi.it; marco.cazzaniga@guest.unimi.it; michele.ceotto@unimi.it

Abstract

In this perspective we show that semiclassical methods provide a rigorous hierarchical way to study the vibrational spectroscopy and kinetics of complex molecular systems. The time averaged approach to spectroscopy and the semiclassical transition state theory for kinetics, which have been first adopted and then further developed in our group, provide accurate quantum results on rigorous physical grounds and can be applied even when dealing with a large number of degrees of freedom. In spectroscopy, the multiple coherent, divide-and-conquer, and adiabatically switched semiclassical approaches have practically permitted to overcome issues related to the convergence of results. In this perspective we demonstrate the possibility to study the semiclassical vibrational spectroscopy of a molecule adsorbed on an anatase (101) surface, a system made of 51 atoms. In kinetics, the semiclassical transition state theory is able to

account for anharmonicity and the coupling between the reactive and bound modes. Our group has developed this technique for practical applications involving the study of phenomena like kinetic isotope effect, heavy atom tunneling, and elusive conformer lifetimes. Here, we show that our multidimensional anharmonic quantum approach is able to tackle on-the-fly the thermal kinetic rate constant of a 135 degree-of-freedom system. Overall, semiclassical methods open up the possibility to describe at the quantum mechanical level systems characterized by hundreds of degrees of freedom leading to the accurate spectroscopic and kinetic description of biomolecules and complex molecular systems.

Trying to summarize one of the key points reported by William H. Miller in his 2005 PNAS perspective "Quantum dynamics of complex molecular systems",[1] the ultimate goal of semiclassical (SC) dynamics is to get a quantum mechanical description of large dimensional (or complex) systems by exploiting the large-scale feasibilty of classical molecular dynamics simulations. The need for SC dynamics methods was invoked because pure quantum simulations were (and still are) computationally affordable only for small molecules. However, there are instances in which quantum effects are expected to be sizable also for large molecular systems including materials and biochemicals. In his perspective, Miller also suggested that the way to reach the goal was to make SC theory and calculations practical to be interfaced with classical molecular dynamics. In the wake of such a suggestion, in the last 20 years semiclassical dynamics has been developed both theoretically[2–11] and practically[12–18] to make it suitable to tackle different kinds of research topics including spectroscopy of gas-phase and solvated systems,[19–25] kinetics,[26–30] and wavefunction calculations.[31–33]

In this perspective we describe semiclassical spectroscopy and kinetics giving an overview of recent accomplishments in our group. We point out the advances achieved with reference to Miller's perspective, and demonstrate the effectiveness of semiclassical techniques. We also suggest a few steps we think should be taken next in the field.

We start our perspective from spectroscopy, and, specifically, we focus on vibrational spec-

troscopy. Vibrational spectroscopy is a quantum mechanical topic related to light-induced or light-stimulated transitions between vibrational energy levels. Several quantum mechanical approaches have been developed to perform spectroscopy simulations. They can be divided into two groups, depending on if they rely on a time-independent approach or a time-dependent one. Without expectation of being exhaustive and with no aim of giving a review of the many studies in theoretical vibrational spectroscopy, we mention the vibrational configuration interaction (VCI) method[34–36] and the second-order vibrational perturbation theory (VPT2)[37,38] as examples of time-independent approaches. A time-dependent approach to spectroscopy relies on appropriate correlation functions, as described by Heller discussing semiclassical spectroscopy.[39] Besides semiclassical spectroscopy, other time-dependent approaches include the multi configuration time dependent Hartree method (MCTDH),[40,41] ring-polymer (RPMD)[42] and centroid (CMD)[43] molecular dynamics, quasi-classical (trajectory) molecular dynamics (QCT)[44] and classical molecular dynamics,[45,46] even though the last two are classical in nature, and they are not able to account for quantum dynamical effects.

The quantity which is straightforward to calculate by means of semiclassical spectroscopy is the quantum density of vibrational states (I(E), E being the vibrational energy). This is obtained as the Fourier transform of the survival amplitude of an arbitrary quantum wavepacket $|\Psi\rangle$

$$I(E) = \frac{1}{2\pi\hbar} \int e^{iEt/\hbar} \langle \Psi(0)|\Psi(t)\rangle \, dt. \tag{1}$$

Eq.(1) defines the power spectrum, which provides the set of all vibrational eigenvalues on an absolute scale. The quantum propagation in Eq.(1) can be approximated semiclassically by means of the Herman-Kluk propagator leading to well-known convergence issues (i.e. the so-called sign problem). The problem was largely overcome by means of the time average technique introduced by Kaledin and Miller in 2003[47] owing to the positive-definite integrand in their formulation, i.e.

$$I(E) = \frac{1}{(2\pi\hbar)^F} \int d\mathbf{p}_0 d\mathbf{q}_0 \frac{1}{2\pi\hbar T} \left| \int_0^T dt\, e^{i[S_t(\mathbf{p}_0,\mathbf{q}_0)+Et+\phi(\mathbf{p}_0,\mathbf{q}_0)]/\hbar} \langle \Psi | \mathbf{p}_t, \mathbf{q}_t \rangle \right|^2 . \qquad (2)$$

In Eq.2 all quantities are obtained from classical trajectory dynamics started with initial momenta $\mathbf{p}_0$ and positions $\mathbf{q}_0$. Specifically, F indicates the number of vibrational degrees of freedom, S($\mathbf{p}_0$,$\mathbf{q}_0$) is the classical action, ϕ($\mathbf{p}_0$,$\mathbf{q}_0$) is the phase of the Herman-Kluk prefactor, and $|\mathbf{p}_t, \mathbf{q}_t\rangle$ is a coherent state evaluated at time t. The phase of the Herman-Kluk prefactor ϕ($\mathbf{p}_0$,$\mathbf{q}_0$) is related to the classical stability matrix and defined as

$$\phi(\mathbf{p}_0, \mathbf{q}_0) = \text{phase} \left[\sqrt{\left| \frac{1}{2} \left(\frac{\partial \mathbf{q}_t}{\partial \mathbf{q}_0} + \mathbf{\Gamma}^{-1} \frac{\partial \mathbf{p}_t}{\partial \mathbf{p}_0} \mathbf{\Gamma} - i\hbar \frac{\partial \mathbf{q}_t}{\partial \mathbf{p}_0} \mathbf{\Gamma} + \frac{i}{\hbar} \mathbf{\Gamma}^{-1} \frac{\partial \mathbf{p}_t}{\partial \mathbf{q}_0} \right) \right|} \right] , \qquad (3)$$

where $\mathbf{\Gamma}$ is commonly a diagonal width matrix with elements equal to the harmonic frequencies of vibration. Kaledin and Miller were able to calculate the vibrational levels and power spectra of small molecules, like water and methane, by means of Eq.(2). Despite the advances obtained with such an approach, further progress was needed to deal with more complex systems. There were three major issues to be faced: i) a spectroscopically accurate analytical potential energy surface (PES) on which to perform the dynamics is generally not available for large molecular systems, so one has to employ the more computationally intensive *ab initio* molecular dynamics. The consequence is that just a handful of trajectories can be evolved and they should be tailored in a way to reproduce the results of a fully converged calculation as accurately as possible; ii) The $\langle \Psi | \mathbf{p}_t, \mathbf{q}_t \rangle$ term, which appears in Eq.(2), is less and less likely to return a sizeable signal along the entire trajectory as the dimensionality of the system increases; iii) classical dynamics is generally chaotic leading to numerical instability of the calculation.

The first issue is related to the need to employ as few trajectories as possible. This is because semiclassical methods require to compute also the Hessian matrix along the trajectory and, when operating with *ab initio* "on-the-fly" dynamics, the computational overhead is huge even when adopting schemes to reduce the number of necessary Hessian calcula-

tions.[16,48,49] The problem has been solved by means of the multiple coherent semiclassical initial value representation (MC SCIVR).[12] The assumption at the heart of the MC-SCIVR method is that vibrational eigenvalues can be obtained from a single trajectory provided it is run at an energy in the neighborhood of the true (but unknown) quantum one. This was also previously demonstrated for low dimensional systems by De Leon and Heller employing a trajectory of energy exactly equal to the quantum vibrational energy under study.[50] In MC SCIVR the initial phase space conditions (i.e. $\mathbf{p}_0, \mathbf{q}_0$) are chosen to be the equilibrium molecular geometry ($\mathbf{q}_{eq}$) and momentum components derived from the harmonic approximation of the vibrational frequency that one wants to simulate, i.e. $p_{i,\mathrm{eq}} = \sqrt{(2n+1)\hbar\omega_i}$, where ω_i is the harmonic frequency of the i-th normal mode and n is determined by the vibrational state of interest. In addition, one chooses a reference state $|\psi\rangle$ as an appropriate combination of coherent states based on $\mathbf{p}_{eq}, \mathbf{q}_{eq}$ in a way to enhance the Fourier transform signal of the vibrational peak of interest.

It is worth noticing that the possibility to employ a single trajectory is also typical of a different semiclassical approach known as thawed Gaussian wavepacket dynamics (TGWD). In TGWD a Gaussian ansatz is inserted in the time-dependent Schroedinger equation and equations of motion for the wavepacket are derived, including one for the width matrix. Once the time evolution of the wavepacket has been integrated, correlation functions can be calculated. TGWD is still actively being advanced theoretically and employed in cutting-edge applications for instance to vibronic spectroscopy.[21,51,52]

The second issue is related to the possibility to get a sensible spectroscopic signal when the dimensionality of the system increases beyond 20-30 degrees of freedom. To overcome this problem, our group has developed the divide-and-conquer semiclassical initial value representation (DC SCIVR) method.[6,53] Starting from the MC-SCIVR single-trajectory approach, Eq.(2) can be projected onto subspaces and written down, for each subspace, as

$$\tilde{I}(E) = \left(\frac{1}{2\pi\hbar}\right)^F \frac{1}{2\pi\hbar T} \left| \int_0^T dt \langle \tilde{\mathbf{p}}_{eq}, \tilde{\mathbf{q}}_{eq} | \tilde{\mathbf{p}}_t, \tilde{\mathbf{q}}_t \rangle e^{i[\tilde{S}_t(\tilde{\mathbf{p}}_{eq}, \tilde{\mathbf{q}}_{eq}) + Et + \tilde{\phi}_t]/\hbar} \right|^2, \tag{4}$$

where the tilde symbol ($\sim$) indicates a subspace-projected quantity and the reference state $|\tilde{\mathbf{p}}_{eq}, \tilde{\mathbf{q}}_{eq}\rangle$ has been chosen according to the MC-SCIVR recipe. All projected terms are straightforward to obtain from the dynamics, with the exception of $\tilde{S}$ which needs calculation of a projected potential. In practice, the modes of vibration are partitioned into subspaces in which the semiclassical calculation is performed by means of Eq. (4). The instantaneous projected potential is defined as $\tilde{V}_S = V(\tilde{q}_{\tilde{N}}; q_{F-\tilde{N}}) - V(\tilde{q}_{\tilde{N},eq}; q_{F-\tilde{N}})$, where the $\tilde{N}$ configurations in the subspace under investigation are considered once instantaneously and once at equilibrium, while the remaining $F - \tilde{N}$ degrees of freedom act as parameters at their instantaneous configuration. The coupling between modes belonging to different subspaces is still accounted for (in an approximate way) by means of the full-dimensional dynamics.

Classical trajectories are not problematic when the number of degrees of freedom increases, since classical evolutions are computationally affordable even for very large systems. However, classical mechanics is chaotic and this leads to numerical instability of the Herman Kluk pre-factor. To alleviate this problem we have developed the adiabatically switched semiclassical initial value representation (AS SCIVR).[8,54,55] The approach is based on two consecutive dynamics runs. The first run is the adiabatic switching one: one or more trajectories (depending on whether the potential is calculated on-the-fly and *ab initio* or not) are started from the usual harmonically-quantized initial conditions of MC SCIVR, and the true vibrational Hamiltonian is switched on very slowly. In this way, based on the adiabatic theorem, quantization is (approximately) maintained for the actual system. The final geometries and momenta of this first run serve as initial conditions for the second run. The second run is simply an SCIVR simulation, with possibility to employ the DC-SCIVR technique. Adoption of the AS-SCIVR method allows to increase the number of degrees of freedom which can be treated in full dimensionality.

Over the years, a hierarchical development of semiclassical spectroscopy methods has been undertaken.Thanks to these advances, almost 20 years after Miller's PNAS perspec-

tive, the ground has been set for studying the spectroscopy of complex systems like those involved in microsolvation, solvation, and materials chemistry. We have already contributed to some pioneering applications of semiclassical methods to glycine microsolvation and liquid water.[24,56] Furthermore, very recently, our group performed a vibrational study of thymidine in explicit bulk water by implementing our DC-SCIVR method in a QM/MM potential energy surface calculation approach.[25] As a demonstration of future routes that semiclassical spectroscopy will be able to take routinely, in the following we report an application to a complex system concerning the vibrational spectroscopy of a molecule interacting with the surface of a material.

We performed an on-the-fly DC-SCIVR calculation for N_2O adsorbed on the TiO_2 anatase (101) surface based on DFT-PBE level of theory for the potential energy. Calculations were undertaken using a plane-wave and pseudopotential approach as implemented in the Quantum-Espresso suite of codes[57,58]. In the calculations we adopted ultrasoft pseudopotentials with an energy cutoff of 60 Ry for the wavefunctions and 480 Ry for the electronic density, while the Brillouin zone was sampled adopting only the Γ-point. The (101) surface was generated starting from the theoretical TiO_2 lattice parameters. It was made of 4 Ti atomic layers with the two deepest ones fixed at the bulk position and exposing 4 potential adsorption sites (Ti_{5C} atoms) to the surface. A vacuum separation of 9 Å was inserted between periodic slab replicas. A total of 51 atoms (48 for the surface plus 3 for the interacting molecule) were employed in the simulation.

For the present discussion, we report the frequencies obtained at the harmonic level through a Density Functional Perturbation Theory (DFPT) calculation, and anharmonic frequency estimates from QCT and DC-SCIVR calculations based on a NVE Born-Oppenheimer molecular dynamics. The calculated single trajectory was made of 2500 steps of 10 a.u. each (for a total evolution of about 0.6 ps), and it was integrated by means of a velocity-Verlet algorithm. To determine the subspace partition for the DC-SCIVR calculation we adopted the procedure reported in Ref. 59,60 using 20 full dimensional Hessians along the trajectory.

A 4-dimensional subspace including the bending and stretch modes of the adsorbed N_2O was selected and, consequently, the Hessians along the trajectory (computed by finite difference of the forces in normal mode coordinates) and the projected potentials were determined for these 4 vibrational modes. Similarly, for the gas-phase molecule we performed a full (4-) dimensional calculation using the same procedure employed for adsorbed molecules to determine the Hessians along the trajectory.

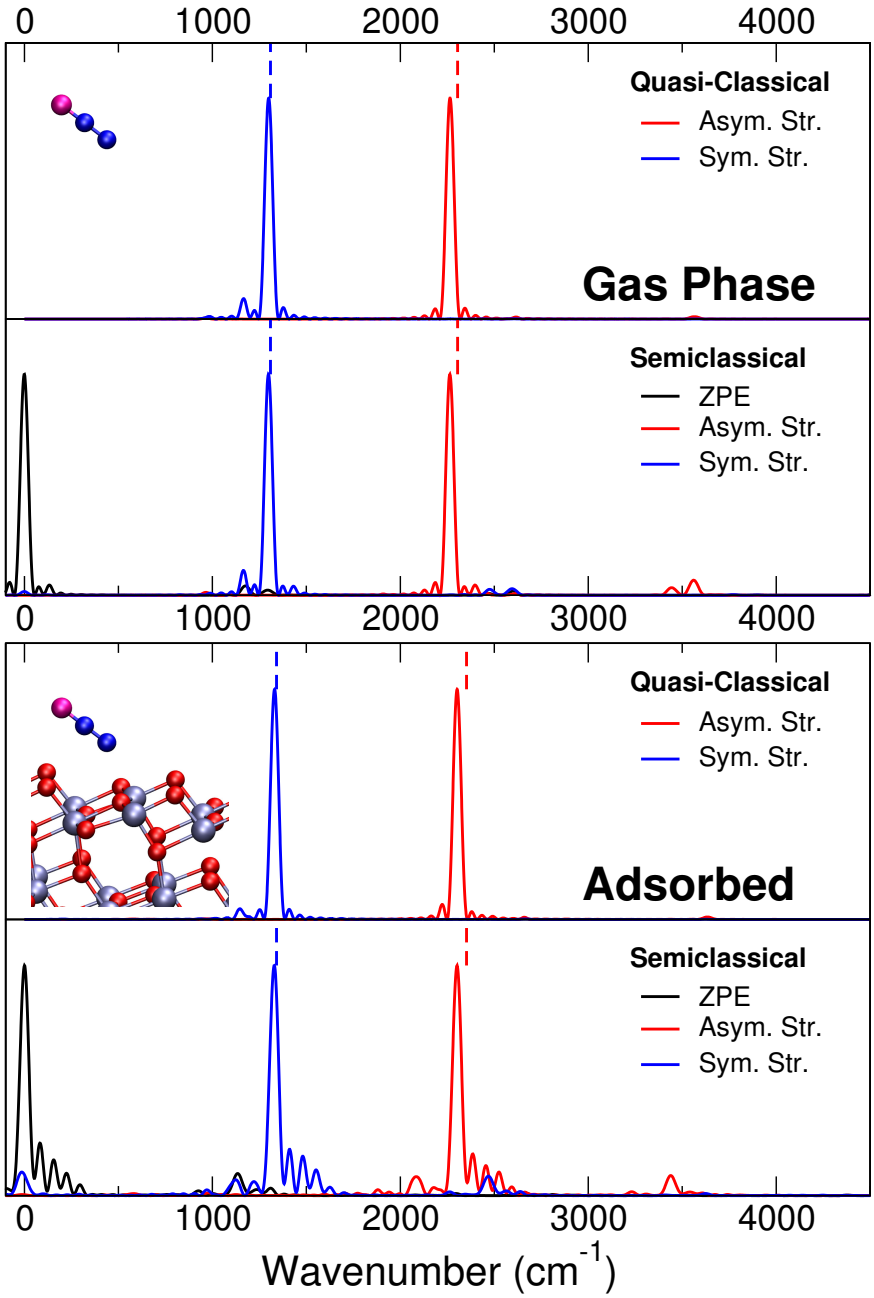

Figure 1: Comparison of QCT and SC power spectra for N_2O in gas phase and upon adsorption on the TiO_2 anatase (101) surface. Harmonic values are reported for reference as dashed lines. Blue spectra are focused on the symmetric stretch, while red spectra on the asymmetric stretch. For the sake of comparison, for the SC spectra the ZPE has been shifted to 0.

Fig. 1 shows a comparison between harmonic, QCT and SC calculations for both gas-phase and adsorbed N_2O. QCT results obtained on longer trajectories were employed for

comparison to experimental results in a previous paper by two of us.[61] It is evident and noteworthy that the SC calculations are able to point out a number of additional features compared to the QCT ones, allowing one to best understand the underlying physics of the system. Spectra presented in Fig. 1 focus on the two stretching modes of N_2O. Therefore, they mainly point out spectral features related to the stretches and modes coupled to them. The bending modes have frequencies comparable to those of the anatase surface: They are degenerate at about 590 cm^{-1} for the gas phase, and nearly degenerate for the adsorbed molecule (579 cm^{-1} e 587 cm^{-1}). Table 1 reports a comparison of the fundamental frequencies of the two stretching modes estimated with different approaches.

Table 1: Comparison of fundamental vibrational frequencies of N_2O in gas phase and upon adsorption on the TiO_2 anatase (101) surface computed with different approaches. All the frequencies are in cm^{-1}.

	Asymmetric Stretch	Symmetric Stretch
	Gas phase	
Harmonic	2305	1309
QCT	2265	1300
DC SCIVR	2264	1298
	Adsorbed	
Harmonic	2352	1341
QCT	2302	1331
DC SCIVR	2302	1330

By looking at the SC spectrum for the gas-phase molecule, one can assign a set of spectral features. The bending overtone is estimated at 1166 cm^{-1}, involved in a Fermi resonance with the fundamental frequency of the symmetric stretch, which explains the absence of a neat red shift of the latter compared to the harmonic estimate (1298 vs 1309 cm^{-1}). The fundamental transition for the asymmetric stretch is dominating at 2264 cm^{-1}, while a couple of interesting features appears at 2476 cm^{-1} and 2594 cm^{-1}. These are assigned to the combination of the symmetric stretch with the bending overtone and to the overtone of the symmetric stretch, respectively. Finally, at 3444 $cm^{-1}$and 3560 $cm^{-1}$the combination of asymmetric stretch with the bending overtone and the combination of symmetric and asymmetric

stretches are located.

Moving to the SC spectrum for the adsorbed molecule, we notice that some new features are present, while others that were present in the gas-phase spectrum are quenched in the adsorbed one. Specifically, at around 1124 cm^{-1} the bending overtone is found. The fundamental transition for the symmetric and asymmetric stretches are located at 1330 $cm^{-1}$and 2302 cm^{-1}, respectively. Remarkably, both of them are associated with a series of close peaks which reflect the low-frequency modes of the surface coupled with the molecule. Combination of symmetric stretch and bending overtone is at 2468 cm^{-1}, and combination of asymmetric stretch and bending overtone is at 3438 cm^{-1}. Semiclassical results are summarized in Table2, where one can appreciate how the adsorption process is not simply inducing red shifts compared to the gas phase vibrational frequencies but also less intuitive blue shifts.

Table 2: SC energy levels for N_2O in gas phase and adsorbed on TiO_2 anatase. The ground state (ZPE) energy has been set to 0. Mode notation is taken from the harmonic description of the isolated molecule, i.e. (n_s,n_b,n_a), where n_s is the quantum number for the symmetric stretch, n_b for the bending, and n_a for the asymmetric stretch. Values are in cm^{-1}.

mode	SC gas-phase	SC adsorbed	Adsorption shift
(0,2,0)	1166	1124	-42
(1,0,0)	1298	1330	+32
(0,0,1)	2264	2302	+38
(1,2,0)	2476	2468	-8
(2,0,0)	2594	-	-
(0,2,1)	3444	3438	-6
(1,0,1)	3560	-	-

As a final perspective of semiclassical vibrational spectroscopy, we notice that there is a theoretical aspect that can be still developed. It is represented by the possibility to simulate actual IR spectra by calculating accurately the intensity of the vibrational transitions in addition to their frequency. To this end, two possible semiclassical approaches have already been presented by our group, one starting from calculations of semiclassical vibrational wavefunctions and another one taking advantage of the power spectrum lineshape.[31,62] Even

if both of them originate from power spectrum calculations, it would be more straighforward and portable to different systems to work out an expression for IR absorption directly related to the time averaged version of SC spectroscopy. In this regard, the absorption lineshape ($\sigma(\omega)$) at temperature T can be calculated as the Fourier transform of a dipole dipole correlation function. In quantum mechanical terms this is the Fourier transform of a trace

$$\sigma(\omega) = \frac{1}{2\pi}\int_{-\infty}^{+\infty} e^{-i\omega t}\mathrm{Tr}\left[\frac{e^{-\beta\hat{H}}}{Q}\hat{\mu}e^{i\hat{H}t/\hbar}\hat{\mu}e^{-i\hat{H}t/\hbar}\right]dt, \tag{5}$$

where Q is the quantum partition function of the system, $\beta = 1/T$ is the Boltzmann constant, $\hat{\mu}$ is the electric dipole operator, and $\hat{H}$ is the vibrational Hamiltonian operator. The corresponding IR absorption spectrum ($\alpha(\omega)$) at temperature T is obtained as

$$\alpha(\omega) = \omega(1 - e^{-\beta\hbar\omega})\sigma(\omega). \tag{6}$$

Demonstration of how to work out a time averaged expression for $\sigma(\omega)$, and therefore $\alpha(\omega)$, with some relevant applications to some molecules is the object of a recent paper.[63] What is important to notice in this Perspective is that this new approach opens up the possibility to adopt the same techniques developed for SC power spectra (i.e. MC SCIVR, DC SCIVR, and AS SCIVR) for calculation of IR spectra. In this way, semiclassical IR spectra are potentially envisioned to be available in the near future for biomolecules, solvated systems, and materials at the same level of accuracy already demonstrated for power spectra. We think this advance will be fundamental for a better interpretation of spectroscopy experiments of complex molecular systems.

Fig. 2 presents a summary of the different techniques developed for semiclassical spectroscopy and their main associated features. Specifically, we want to stress how the Herman-Kluk SC IVR approximation can present several levels of approximation and computational demands, and that both power and IR spectra can be simulated. Within the SC IVR approach, one always knows the hierarchical level of the semiclassical method employed.

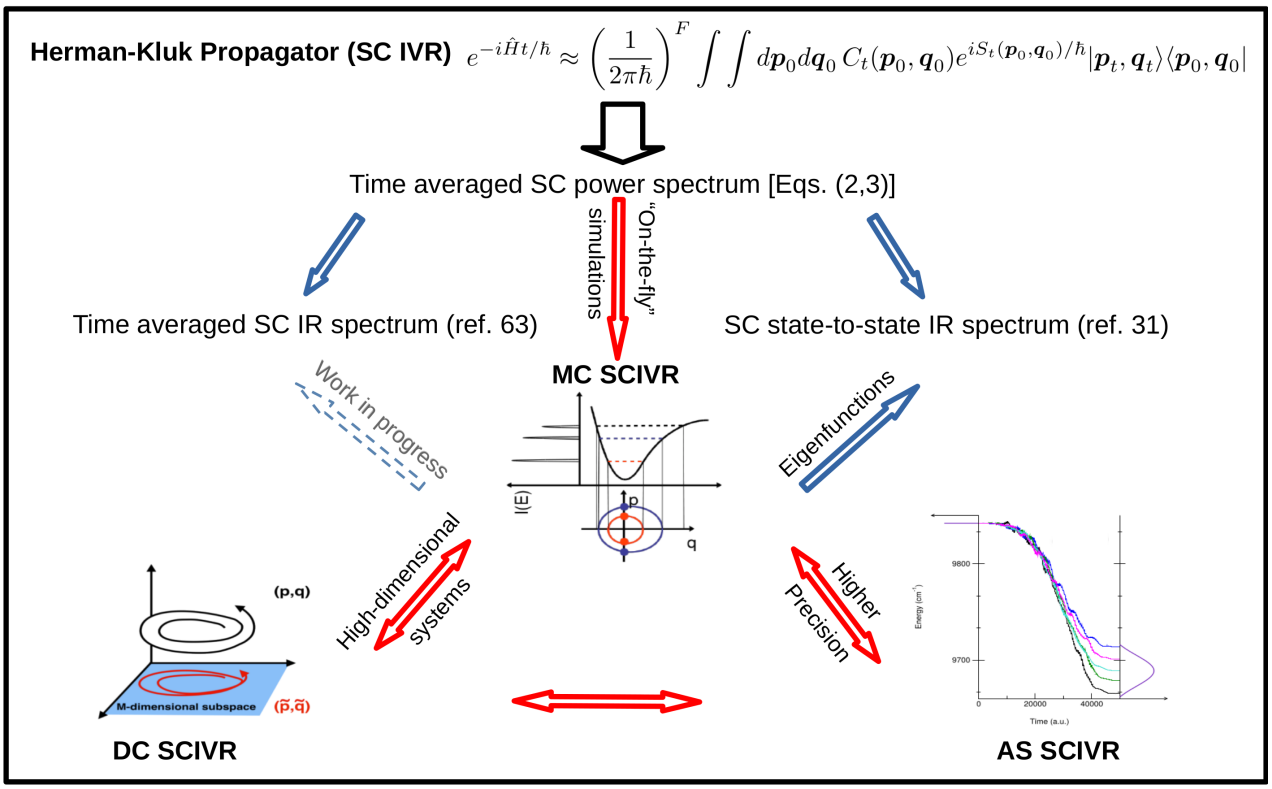

Figure 2: Scheme of different techniques for semiclassical spectroscopy

Beyond spectroscopy, another field in which SC methods have been widely developed and adopted is the kinetic one, with focus on the calculation of thermal rate constants. There are basically two semiclassical approaches to the calculation of reaction rates. One is based on the semiclassically approximate simulation of the quantum dynamics of the reaction[4,64–67] and the other one on zero-time or Transition State Theory-like approximations.[27,68–76] The first approach is still nowadays a challenging task in theoretical chemistry usually applicable only to model systems, while the second one is more practical. Among the techniques included in the second group, there is the semiclassical transition state theory (SCTST) introduced by Miller in the early 1970s[77] and later revised by Miller and Hernandez in the 1990s.[78,79] This approach is attractive because it requires only local information about the Transition State (TS) on the PES, as well as basic input quantities that are routinely calculated by standard quantum chemistry codes, such as the harmonic vibrational frequencies, VPT2 anharmonic coupling constants between modes, and the height of the reaction barrier. In

the past years, in our group, SCTST has been implemented in a way that it can now be conveniently applied to high dimensional systems and it is possible to reach coupled cluster *ab initio* accuracy for smaller systems, as explained below. Therefore, in a similar way to spectroscopy, also in the kinetic field SC methods have recently moved to the investigation of large systems as foreseen in Miller's perspective. Recently, applicability of SCTST to large systems has attracted the interest of other research groups too, who have been involved in the development of reduced-dimensionality approaches.[80]

One could think that a classical dynamics time-dependent flux calculation across a dividing surface between reactants and products associated to a Monte Carlo phase space sampling would be often enough for rate calculations. However, a proper multidimensional treatment of quantum effects is necessary for a successful comparison with experimental results, sometimes even at room temperatures.[74] Furthermore, as we will report below, quantum effects are not limited to light atom transfer. Consequently, it is vital to have a method, SCTST, that can recover quantum effects, such as tunneling and zero point energy contributions, in a non-empirical fashion and without requiring separability of the degrees of freedom along any multidimensional reaction path.[81] SCTST is by far more accurate than standard TST corrections, such as Wigner or Eckart corrections,[82] which are based on one-dimensional tunneling corrections along the reaction path and cannot get, for example, corner-cutting tunneling effects. Instead, in SCTST all degrees of freedom are equally accounted for as demonstrated by the excellent agreement to experimental results or exact (when available) quantum mechanical calculations for a series of small size reactive systems.[83]

To appreciate the semiclassical flavor of the SCTST method and the effectiveness of the most recent advances, we start from the exact quantum mechanical kinetic rate constant[68,77,84]

$$k(T) = \frac{1}{2\pi\hbar Q_r} \int N_{QM}(E) e^{-\beta E} dE, \tag{7}$$

where $N_{QM}(E)$ is the amount of reactant density converted into products at a given E value, i.e. the exact quantum Cumulative Reaction Probability (CRP), $\beta = 1/(k_B T)$ where T and

k_B are respectively the temperature and the Boltzmann constant. The SCTST approximation consists in taking the following multidimensional Wentzel–Kramers–Brillouin (WKB) CRP approximation[85]

$$N_{QM}(E) = \sum_{\mathbf{n}=0} P_n(E) \approx \sum_{\mathbf{n}=0} \left[1 + e^{2\Theta(E,\mathbf{n})}\right]^{-1} = N(E), \tag{8}$$

where $\sum_{\mathbf{n}=0} = \sum_{n_1=0} \sum_{n_2=0} \cdots \sum_{n_{N-1}=0}$ is the sum over all vibrational quantum numbers of the N-1 bound modes and $\Theta(E, \mathbf{n})$ is the multidimensional barrier penetration integral. E depends on all quantum numbers (the ones for the bound modes $\mathbf{n}$ and the one for the reactive mode n_N). Since the action variable for the reactive mode is imaginary and can be assumed in a Bohr-Sommerfeld fashion to be $\left(n_N + \frac{1}{2}\right) = \frac{i\Theta}{\pi}$,[86] the total energy can be written also as a function of the penetration integral $\mathrm{E}(\boldsymbol{n}, \Theta)$. To obtain an explicit expression for Θ, Miller and Hernandez assumed a standard perturbative expression for the vibrational energy levels also at the stationary TST point[78]

$$E(n_1, \ldots, n_N) = V_0 + \sum_{k=1}^{N} \hbar\omega_k (n_k + \frac{1}{2}) + \sum_{k \le k'}^{N} \chi_{kk'} (n_k + \frac{1}{2})(n_{k'} + \frac{1}{2}), \tag{9}$$

where V_0 is the potential energy at the stationary point, ω_k are the harmonic frequencies, and $\chi_{kk'}$ are the anharmonic constants. In this way, the penetration integral Θ is obtained by inverting Eq. 9 after assuming the Bohr-Sommerfeld relation for n_N

$$\Theta(n_1, ..., n_{N-1}, E) = \frac{\pi \Delta E}{\hbar \Omega_N} \frac{2}{1 + [1 + 4\chi_{NN}\Delta E/(\hbar\Omega_N)^2]^{\frac{1}{2}}} \tag{10}$$

where

$$\begin{aligned} \Delta E &= V_0 - E + \sum_{k=1}^{N-1} \hbar\omega_k (n_k + \frac{1}{2}) + \sum_{k \le k'}^{N-1} \chi_{kk'} (n_k + \frac{1}{2})(n_{k'} + \frac{1}{2}) \\ \hbar\Omega_N &= \hbar\tilde{\omega}_N - \sum_{k=1}^{N-1} \tilde{\chi}_{kN} (n_k + \frac{1}{2}). \end{aligned} \tag{11}$$

For the reactive mode we have that $\omega_N = i\tilde{\omega}_N$ and $\chi_{kN} = -i\tilde{\chi}_{kN}$. Eq. 10 allows to evaluate the sum in Eq 8 and to get the reaction rate from Eq.7 in the semiclassical approximation. More specifically, the SCTST expression we employ for the thermal rate constant is

$$k(T) = \frac{1}{h}\frac{Q_{TS}^{tra}}{Q_R^{tra}}\frac{Q_{TS}^{rot}}{Q_R^{rot}}\frac{\int_0^{+\infty} N(E)e^{-\beta E}dE}{Q_R^{vib}}, \tag{12}$$

where we consider the overall translation and rotations as separable. Q^{rot} is the rotational partition function and Q^{tra} is the translational one, approximated to

$$\begin{aligned} Q^{rot} &= \frac{\sqrt{\pi}}{s}\prod_{\alpha}\left(\sqrt{8\pi^2 I_\alpha \frac{k_b T}{h^2}}\right), \\ Q^{tra} &= \left(\frac{2\pi M k_b T}{h^2}\right)^{\frac{3}{2}} \end{aligned} \tag{13}$$

respectively, where s is the rotational symmetry number, I_α is the moment of inertia along the α axis and M is the mass. Furthermore, the reactant vibrational partition function is calculated by including anharmonic effects and fully coupling all the degrees of freedom by employing the Density Of vibrational States (DOS) $\rho(E_v)$:

$$Q_R^{vib}(T) = \int_0^{+\infty} \rho(E_v)e^{-\beta E_v}dE_v. \tag{14}$$

A practical way to calculate $N(E)$ in Eq.12 is

$$N(E) = \sum_{j=1}^{E/\delta E} \delta E \rho^{\dagger}(E_j) \langle P(E_j)\rangle, \tag{15}$$

where the energy range has been discretized into bins of width δE.[87] $\delta E\rho^{\dagger}(E_j)$ is the number of states in the j-th energy bin, and

$$\langle P(E_j)\rangle = \frac{\sum_{\boldsymbol{n}} P_{\boldsymbol{n}}(E_j)}{\#_j} \tag{16}$$

is the average reaction probability in the j-th energy bin which contains a number $\#_j$ of energy levels identified by a suitable combination of quantum numbers $\mathbf{n}$. Each $P_{\boldsymbol{n}}(E_j)$ is calculated from the Θ corresponding to each $\mathbf{n}$. In Eq. 15 $\rho^{\dagger}(E_j)$ is the vibrational density of states (DOS) of the bound states at the TS.

The two more computationally intensive tasks, which have hampered application of SCTST to complex systems in the past, are the calculation of the vibrational state density at reactant and TS geometry in Eqs. 14 and 15, and the calculation of the anharmonic constants $\chi_{kk'}$ in the energy expansion 9. In recent years, our group focused on drastically reducing the computational cost of SCTST calculations by exploiting computational parallel architectures.[30,88–90]

The vibrational density of states can be calculated using the Wang-Landau (WL) algorithm.[87,91,92] According to the WL algorithm, a random walk is performed in the space of quantum number combinations $\mathbf{n}$ over an energy range (relative to the bound state ZPE) sufficiently large to account for the infinite limit of integration in Eq. 12. The energy range is discretized into energy bins and a histogram of visits of each energy bin is recorded during the random walk. According to the WL prescription for the probability of accepting a new move,[92] if the histogram is flat, then the probability of visiting each energy bin is proportional to $1/\rho(E_j)$. Thus, our parallelization strategy consist in taking advantage of the MPI (Message Passing Interface) API (Application Programming Interface) and dividing the energy range into windows. Calculations of the density of states are processed independently on a single CPU processor for each random walker in each window. Furthermore, calculations of the density of states are processed independently for each energy window. When convergence is achieved within each window, the overall density of states on the complete energy range is recovered by matching the estimates obtained in each window. The partial density of states is renormalized in a cascade starting from the lowest energy window (where it is assumed that the first energy bin contains just the ZPE state) by means of an overlap between subsequent windows.[89,93]

Thanks to this implementation we have been able to speed up the calculation of the vibrational density of states of the HOCO radical, N-methylmethanimine (CH_2NCH_3), naphtalene ($C_{10}H_8$), triethylphosphine ($P-(CH_3CH_2)_3$), and anthracene (C_4H_{10}).[89] These species are characterized by a number of vibrational degrees of freedom equal to 6, 18, 48, 60, and 66 respectively. Overall, we observed an almost linear scaling, and we concluded that our parallelization resulted to be absolutely advantageous compared to other codes commonly employed for these type of calculations. Then, we implemented this parallelization in MultiWell,[94,95] a suite of codes originally developed by Barker, which includes SCTST for rate constant calculations. Two of us contributed to Multiwell with *paradensum* and *parsctst* programs.

As a demonstration, here we report a re-elaboration of a previous application of our codes to the calculation of the rate constant of the isomerization reaction of the 2,4,6-tri-tert-butylphenyl to 3,5-di-tert-butylneophyl, a system made of 135 vibrational DOFs.[88] This intermolecular proton transfer reaction is known to experience quantum tunneling at low temperature. Furthermore, electron paramagnetic resonance spectroscopy (EPR) experiments detected a significant tunneling contribution already at 247K. Experimental data are reported in Fig. 3 down to 28 K.[96] In addition, the experiments demonstrated that the type of solvent employed does not affect the reaction rate. We reproduced the strong non-Arrhenius behaviour with a gas phase computational set-up employing UB3LYP/6-311G** + D3 in Gaussian 16[97] for all calculations but the barrier height, i.e. the energy difference between reactants and products, which was refined at MP2/6- 311G** level of theory using the NWChem suite of codes.[98] We observed that, along the minimum energy path, a methyl group rotates around its C-C bond to donate a proton to the phenyl ring before relaxing back by rotating again around the same bond. We found that our parallelization set with uneven energy windows distribution and narrower windows at lower energy was able to reach an almost ideal parallel performance.

In Fig. 3 we report the DFT SCTST results with (blue continuous line) and without

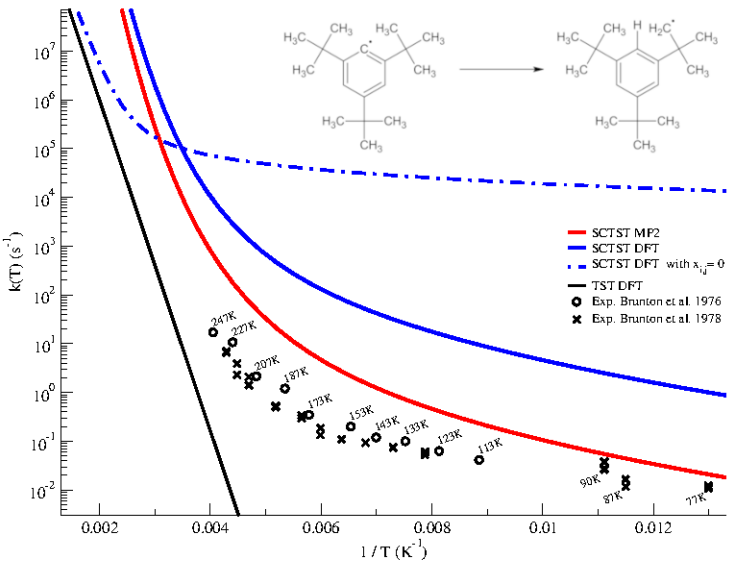

Figure 3: 2,4,6-tri-tert-butylphenyl SCTST rate constant simulations at different level of theory.

(blue dash-dotted line) anharmonic corrections, together with their DFT TST approximation (black continuous line). It is interesting to observe that the inclusion of anharmonic constants is important not only in the tunneling region but also at high temperatures, where high accuracy in the partition function calculation is mandatory. In Fig. 3 the results with the MP2 barrier value (red continuous line) are the most accurate ones. From the results reported in Fig. 3 one can assess that agreement to the experimental results obtained with our semiclassical method, even if still on qualitative grounds, is by far better than the one provided by a traditional TST approach. This better agreement is reached thanks to inclusion of (i) tunneling, (ii) anharmonicity, and (iii) vibrational coupling in the SCTST approach.

We now focus on the significant difference between the DFT results and those corrected by the MP2 barrier. This difference shows the importance of the *ab initio* level of calculation which is probably the reason why we are not able to provide a quantitative agreement in this 135-dimensional example (at least in the shallow tunneling regime). The main bottleneck to the adoption of higher levels of *ab initio* electronic theory is given at this stage by the

anharmonic constants $\chi_{kk'}$ appearing in Eq. 11. Approaches for $\chi_{kk'}$ parallel evaluation were already documented in the literature for spectroscopy applications,[99] and a specific implementation for the coupled cluster level (CC) is given in the Cfour code.[100] We introduced in MultiWell an implementation, named *fdacc*, suitable for multi-node architectures to calculate the derivatives necessary to reproduce each $\chi_{kk'}$ for both mininum and TS structures using finite difference formulas typical of Fornberg schemes.[101] The hallmark of our *fdacc* implementation[90] is that it can be interfaced to any *ab initio* quantum chemistry software at any level of electronic structure theory. It can be employed also for purposes other than rate calculations, such as VPT2 vibrational energy level estimate. In this way we were able to employ CCSD and CCSD(T) *ab initio* methods for the full dimensional rate calculations with an aug-cc-pVDZ basis set up to 16-atom systems.

More specifically, we looked at the cyclobutene ring opening reaction, the cis-1,3,5-hexatriene electrocyclic ring closing reaction, and the [1,5]-Cope rearrangement of the 1,5-hexadiene molecule. These reactions involve 10, 14, and 16 atoms, respectively and are examples of heavy atom tunneling (HAT) processes.[102–105] In this case SCTST results, which show a significant deviation from the Arrhenius linear behavior, were able to support the hypothesis that indeed there are tunneling contributions even at room temperature for reactions involving mainly heavy atom rearrangements. The interested reader can find the details of this study in Ref. 90

Finally, we want to point out that the SCTST method allows us not only to calculate rate constants accurately, but also to gain physical insights into reaction rates. Specifically, by comparing reactions characterized by HAT tunneling, the 2,4,6-tri-tert-butylphenyl reaction mentioned above, and other reactions for which SCTST calculations are doable, we can remark that, in our experience, tunneling contributions are dominant even at room temperature.

Eventually, the advantage of SCTST is that it is an ideal tool for application due to its user-friendly setup. It only requires the knowledge of the local PES region around the

TS location necessary for calculating sufficiently accurate derivatives up to the fourth order. This is in principle attainable with a finite differences approach also at high level of electronic structure theory without the need to evaluate a large portion of the PES. The tools we have developed in our group and distributed open source with the Multiwell program suite make SCTST accessible even to non-specialized users and push its applicability at accurate levels of electronic structure theory for large molecules. As far as the theory is concerned, SCTST has the advantage over other methods to be able to recover the exact leading order term of the $\hbar^2$ expansion of the tunneling transmission coefficient at high temperature. Many other theories for tunneling calculations can just recover its parabolic barrier approximation.[106,107] SCTST is indeed specifically targeted to the inclusion of anharmonic coupling of the reaction coordinate with the orthogonal modes anharmonically described and thus it is accurate in the shallow tunneling and high temperature regime. In comparison with other semiclassical methods like the semiclassical instanton (SCI),[68,108] SCTST does not suffer from the divergence above a crossover temperature. However, SCTST is known to loose accuracy in the deep tunneling regime for asymmetric barriers.[109] Therefore, a future theoretical advance for SCTST will concern the improvement of the method in the regime of deep tunneling. For instance, it has recently been proposed to connect SCTST with SCI, which is accurate in the deep tunneling regime, i.e. at low temperatures, but conversely accounts only for harmonic quantization of the orthogonal modes.[107] As for applications, our next goal is to employ SCTST for large systems like molecules in gas matrices and solvated systems where we can study the importance of the coupling of the reaction coordinate to the environment modes.

We conclude affirming that the semiclassical methods here described, which are unbiased "democratic" ways to add quantum effects to all degrees of freedom, have the potential to be routinely employed for spectroscopy and kinetics (in gas-phase or solution) of complex chemical systems in the near future. This was the main long-term goal that characterized early-day semiclassical dynamics. After several decades, that goal is now much closer to be achieved. If we had to anticipate the main theoretical challenge to be faced in the future

by these methods we would certainly point to their extension to non-adiabatic dynamics. This is a fast growing field, very challenging from both the electronic structure and nuclear dynamics point of view.

Biographies

Riccardo Conte is assistant professor of theoretical chemistry at Università degli Studi di Milano. He received his Ph.D. in chemistry from Scuola Normale Superiore di Pisa (Italy). He held postdoctoral appointments at the Weizmann Institute of Science (Israel), Emory University (USA), and Università degli Studi di Milano (Italy).

Chiara Aieta is currently a Marie Curie "Global" postdoctoral fellow in the groups of Prof. Sharon Hammes-Schiffer (Pricenton University, USA) and Prof. Michele Ceotto (Università degli Studi di Milano, Italy). She previously held researcher and postdoctoral positions at Università degli Studi di Milano (Italy), where she also got her Ph.D. in chemistry.

Marco Cazzaniga is a senior consultant for the Ceotto group. He received his Ph.D. in physics from Università degli Studi di Milano (Italy). He previously held postoctoral positions at Università degli Studi di Milano (Italy) and at Consiglio Nazionale delle Ricerche (CNR, Italy).

Michele Ceotto is an associate professor of theoretical chemistry at Università degli Studi di Milano (Italy), where he has been an ERC Grantee. After a master degree in chemistry and one in physics at Sapienza Università di Roma, he received his Ph.D. in chemistry from University of California at Berkeley in 2005 under the supervision of W. H. Miller and he held a one-year postdoctoral appointment at University of Utah in G. Voth's group.

Acknowledgement

We thank all group members that have contributed over the years to the development of semiclassical dynamics. R.C. and Mi.C. thank Università degli Studi di Milano for funding under project PSR2022_DIP_005_PI_RCONT. C.A. thanks Università degli Studi di Milano for funding under project PSR2022_DIP_005_PI_CAIET. Mi.C. acknowledges financial support from the European Research Council (Grant Agreement No. (647107)—SEMICOMPLEX—ERC-2014-CoG under the European Union's Horizon 2020 and No. 101081361 — SEMISOFT — ERC-2022-POC2 under Horizon Europe research and innovation programme). R.C. and Ma.C. acknowledge the CINECA award IsCa7_CombH2O, under the ISCRA initiative, for the availability of high-performance computing resources and support.

References

(1) Miller, W. H. Quantum dynamics of complex molecular systems. *Proc. Natl. Acad. Sci. USA* **2005**, *102*, 6660–6664.

(2) Grossmann, F. A semiclassical hybrid approach to many particle quantum dynamics. *J. Chem. Phys.* **2006**, *125*, 014111.

(3) Kay, K. G. The Herman–Kluk approximation: Derivation and semiclassical corrections. *Chem. Phys.* **2006**, *322*, 3–12.

(4) Liu, J. Recent advances in the linearized semiclassical initial value representation/classical Wigner model for the thermal correlation function. *International Journal of Quantum Chemistry* **2015**, *115*, 657–670.

(5) Petersen, J.; Pollak, E. Semiclassical initial value representation for the quantum propagator in the Heisenberg interaction representation. *J. Chem. Phys.* **2015**, *143*, 224114.

(6) Ceotto, M.; Di Liberto, G.; Conte, R. Semiclassical "divide-and-conquer" method for spectroscopic calculations of high dimensional molecular systems. *Phys. Rev. Lett.* **2017**, *119*, 010401.

(7) Church, M. S.; Hele, T. J. H.; Ezra, G. S.; Ananth, N. Nonadiabatic semiclassical dynamics in the mixed quantum-classical initial value representation. *J. Chem. Phys.* **2018**, *148*, 102326.

(8) Conte, R.; Parma, L.; Aieta, C.; Rognoni, A.; Ceotto, M. Improved semiclassical dynamics through adiabatic switching trajectory sampling. *J. Chem. Phys.* **2019**, *151*, 214107.

(9) Church, M. S.; Ananth, N. Semiclassical dynamics in the mixed quantum-classical limit. *J. Chem. Phys.* **2019**, *151*, 134109.

(10) Begušić, T.; Vaníček, J. On-the-fly ab initio semiclassical evaluation of vibronic spectra at finite temperature. *J. Chem. Phys.* **2020**, *153*.

(11) Bonnet, L. Semiclassical initial value representation: From Møller to Miller. II. *J. Chem. Phys.* **2023**, *158*.

(12) Ceotto, M.; Atahan, S.; Tantardini, G. F.; Aspuru-Guzik, A. Multiple coherent states for first-principles semiclassical initial value representation molecular dynamics. *J. Chem. Phys.* **2009**, *130*, 234113.

(13) Ceotto, M.; Atahan, S.; Shim, S.; Tantardini, G. F.; Aspuru-Guzik, A. First-principles semiclassical initial value representation molecular dynamics. *Phys. Chem. Chem. Phys.* **2009**, *11*, 3861–3867.

(14) Tatchen, J.; Pollak, E. Semiclassical on-the-fly computation of the S->S1 absorption spectrum of formaldehyde. *J. Chem. Phys.* **2009**, *130*, 041103.

(15) Tamascelli, D.; Dambrosio, F. S.; Conte, R.; Ceotto, M. Graphics processing units accelerated semiclassical initial value representation molecular dynamics. *J. Chem. Phys.* **2014**, *140*, 174109.

(16) Conte, R.; Gabas, F.; Botti, G.; Zhuang, Y.; Ceotto, M. Semiclassical vibrational spectroscopy with Hessian databases. *J. Chem. Phys.* **2019**, *150*.

(17) Begusic, T.; Cordova, M.; Vanicek, J. Single-Hessian thawed Gaussian approximation. *J. Chem. Phys.* **2019**, *150*, 154117.

(18) Zeng, J.-X.; Yang, S.; Zhu, Y.-C.; Fang, W.; Jiang, L.; Wang, E.-G.; Zhang, D. H.; Li, X.-Z. Semiclassical Vibrational Spectroscopy of Real Molecular Systems by Means of Cross-Correlation Filter Diagonalization. *J. Phys. Chem. A* **2023**, *127*, 2902–2911.

(19) Buchholz, M.; Grossmann, F.; Ceotto, M. Application of the mixed time-averaging semiclassical initial value representation method to complex molecular spectra. *J. Chem. Phys.* **2017**, *147*, 164110.

(20) Patoz, A.; Begusic, T.; Vanicek, J. On-the-Fly Ab Initio Semiclassical Evaluation of Absorption Spectra of Polyatomic Molecules beyond the Condon Approximation. *J. Phys. Chem. Lett.* **2018**, *9*, 2367–2372.

(21) Begusic, T.; Roulet, J.; Vanicek, J. On-the-fly ab initio semiclassical evaluation of time-resolved electronic spectra. *J. Chem. Phys.* **2018**, *149*, 244115.

(22) Liu, X.; Liu, J. Critical role of quantum dynamical effects in the Raman spectroscopy of liquid water. *Mol. Phys.* **2018**, *116*, 755–779.

(23) Conte, R.; Ceotto, M. Semiclassical molecular dynamics for spectroscopic calculations. *Quantum Chemistry and Dynamics of Excited States: Methods and Applications* **2020**, 595–628.

(24) Rognoni, A.; Conte, R.; Ceotto, M. How many water molecules are needed to solvate one? *Chem. Sci.* **2021**, *12*, 2060–2064.

(25) Moscato, D.; Mandelli, G.; Bondanza, M.; Lipparini, F.; Conte, R.; Mennucci, B.; Ceotto, M. Unraveling Water Solvation Effects with Quantum Mechanics/Molecular Mechanics Semiclassical Vibrational Spectroscopy: The Case of Thymidine. *J. Am. Chem. Soc.* **2024**, *146*, 8179–8188.

(26) Richardson, J. O. Derivation of instanton rate theory from first principles. *J. Chem. Phys.* **2016**, *144*, 114106.

(27) Richardson, J. O. Microcanonical and thermal instanton rate theory for chemical reactions at all temperatures. *Faraday Discuss.* **2016**, *195*, 49–67.

(28) Richardson, J. O. Ring-polymer instanton theory. *Int. Rev. Phys. Chem.* **2018**, *37*, 171–216.

(29) Aieta, C.; Ceotto, M. A quantum method for thermal rate constant calculations from stationary phase approximation of the thermal flux-flux correlation function integral. *J. Chem. Phys.* **2017**, *146*, 214115.

(30) Mandelli, G.; Corneo, L.; Aieta, C. Coupled Cluster Semiclassical Estimates of Experimental Reaction Rates: The Interconversion of Glycine Conformer VIp to Ip. *J. Phys. Chem. Lett.* **2023**, *14*, 9996–10002.

(31) Micciarelli, M.; Conte, R.; Suarez, J.; Ceotto, M. Anharmonic vibrational eigenfunctions and infrared spectra from semiclassical molecular dynamics. *J. Chem. Phys.* **2018**, *149*, 064115.

(32) Aieta, C.; Micciarelli, M.; Bertaina, G.; Ceotto, M. Anharmonic quantum nuclear densities from full dimensional vibrational eigenfunctions with application to protonated glycine. *Nat. Comm.* **2020**, *11*, 4384.

(33) Aieta, C.; Bertaina, G.; Micciarelli, M.; Ceotto, M. Representing molecular ground and excited vibrational eigenstates with nuclear densities obtained from semiclassical initial value representation molecular dynamics. *J. Chem. Phys.* **2020**, *153*, 214117.

(34) Bowman, J. M.; Carter, S.; Huang, X. MULTIMODE: a code to calculate rovibrational energies of polyatomic molecules. *Int. Rev. Phys. Chem.* **2003**, *22*, 533–549.

(35) Thomsen, B.; Yagi, K.; Christiansen, O. Optimized coordinates in vibrational coupled cluster calculations. *J. Chem. Phys.* **2014**, *140*, 154102.

(36) Mathea, T.; Rauhut, G. Assignment of vibrational states within configuration interaction calculations. *J. Chem. Phys.* **2020**, *152*, 194112.

(37) Barone, V.; Biczysko, M.; Bloino, J.; Borkowska-Panek, M.; Carnimeo, I.; Panek, P. Toward anharmonic computations of vibrational spectra for large molecular systems. *Int. J. Quantum Chem.* **2011**, *112*, 2185–2200.

(38) Yang, Q.; Bloino, J. An Effective and Automated Processing of Resonances in Vibrational Perturbation Theory Applied to Spectroscopy. *J. Phys. Chem. A* **2022**, *126*, 9276–9302.

(39) Heller, E. J. The semiclassical way to molecular spectroscopy. *Acc. Chem. Res.* **1981**, *14*, 368–375.

(40) Meyer, H.-D.; Manthe, U.; Cederbaum, L. S. The multi-configurational time-dependent Hartree approach. *Chem. Phys. Lett.* **1990**, *165*, 73–78.

(41) Picconi, D.; Cina, J. A.; Burghardt, I. Quantum dynamics and spectroscopy of dihalogens in solid matrices. I. Efficient simulation of the photodynamics of the embedded I2Kr18 cluster using the G-MCTDH method. *J. Chem. Phys.* **2019**, *150*, 064111.

(42) Begušić, T.; Tao, X.; Blake, G. A.; Miller, T. F. Equilibrium–nonequilibrium ring-polymer molecular dynamics for nonlinear spectroscopy. *J. Chem. Phys.* **2022**, *156*.

(43) Rossi, M.; Liu, H.; Paesani, F.; Bowman, J.; Ceriotti, M. Communication: On the consistency of approximate quantum dynamics simulation methods for vibrational spectra in the condensed phase. *J. Chem. Phys.* **2014**, *141*.

(44) Qu, C.; Bowman, J. M. IR Spectra of (HCOOH)2 and (DCOOH)2: Experiment, VSCF/VCI, and Ab Initio Molecular Dynamics Calculations Using Full-Dimensional Potential and Dipole Moment Surfaces. *J. Phys. Chem. Lett.* **2018**, *9*, 2604–2610.

(45) Marx, D.; Hutter, J. *Ab initio molecular dynamics: basic theory and advanced methods*; Cambridge University Press, 2009.

(46) Mathias, G.; Ivanov, S. D.; Witt, A.; Baer, M. D.; Marx, D. Infrared Spectroscopy of Fluxional Molecules from (ab Initio) Molecular Dynamics: Resolving Large-Amplitude Motion, Multiple Conformations, and Permutational Symmetries. *J. Chem. Theory Comput.* **2011**, *8*, 224–234.

(47) Kaledin, A. L.; Miller, W. H. Time averaging the semiclassical initial value representation for the calculation of vibrational energy levels. *J. Chem. Phys.* **2003**, *118*, 7174–7182.

(48) Zhuang, Y.; Siebert, M. R.; Hase, W. L.; Kay, K. G.; Ceotto, M. Evaluating the Accuracy of Hessian Approximations for Direct Dynamics Simulations. *J. Chem. Theory Comput.* **2012**, *9*, 54–64.

(49) Ceotto, M.; Zhuang, Y.; Hase, W. L. Accelerated direct semiclassical molecular dynamics using a compact finite difference Hessian scheme. *J. Chem. Phys.* **2013**, *138*, 054116.

(50) De Leon, N.; Heller, E. J. Semiclassical quantization and extraction of eigenfunctions using arbitrary trajectories. *J. Chem. Phys.* **1983**, *78*, 4005–4017.

(51) Begušić, T.; Vaníček, J. On-the-fly ab initio semiclassical evaluation of vibronic spectra at finite temperature. *J. Chem. Phys.* **2020**, *153*.

(52) JL Vaníček, J. Family of Gaussian wavepacket dynamics methods from the perspective of a nonlinear Schrödinger equation. *J. Chem. Phys.* **2023**, *159*.

(53) Di Liberto, G.; Conte, R.; Ceotto, M. "Divide and conquer" semiclassical molecular dynamics: A practical method for spectroscopic calculations of high dimensional molecular systems. *J. Chem. Phys.* **2018**, *148*, 014307.

(54) Botti, G.; Ceotto, M.; Conte, R. On-the-fly adiabatically switched semiclassical initial value representation molecular dynamics for vibrational spectroscopy of biomolecules. *J. Chem. Phys.* **2021**, *155*, 234102.

(55) Botti, G.; Aieta, C.; Conte, R. The complex vibrational spectrum of proline explained through the adiabatically switched semiclassical initial value representation. *J. Chem. Phys.* **2022**, *156*, 164303.

(56) Schwaab, G.; de Tudela, R. P.; Mani, D.; Pal, N.; Roy, T. K.; Gabas, F.; Conte, R.; Caballero, L. D.; Ceotto, M.; Marx, D., et al. Zwitter ionization of glycine at outer space conditions due to microhydration by six water molecules. *Phys. Rev. Lett.* **2022**, *128*, 033001.

(57) Giannozzi, P.; Baroni, S.; Bonini, N.; Calandra, M.; Car, R.; Cavazzoni, C.; Ceresoli, D.; Chiarotti, G. L.; Cococcioni, M.; Dabo, I., et al. QUANTUM ESPRESSO: a modular and open-source software project for quantum simulations of materials. *J. Phys.: Cond. matt.* **2009**, *21*, 395502.

(58) Giannozzi, P.; Baseggio, O.; Bonfà, P.; Brunato, D.; Car, R.; Carnimeo, I.; Cavazzoni, C.; De Gironcoli, S.; Delugas, P.; Ferrari Ruffino, F., et al. Quantum ESPRESSO toward the exascale. *J. Chem. Phys.* **2020**, *152*.

(59) Cazzaniga, M.; Micciarelli, M.; Moriggi, F.; Mahmoud, A.; Gabas, F.; Ceotto, M. Anharmonic calculations of vibrational spectra for molecular adsorbates: A divide-and-conquer semiclassical molecular dynamics approach. *J. Chem. Phys.* **2020**, *152*, 104104.

(60) Cazzaniga, M.; Micciarelli, M.; Gabas, F.; Finocchi, F.; Ceotto, M. Quantum Anharmonic Calculations of Vibrational Spectra for Water Adsorbed on Titania Anatase (101) Surface: Dissociative versus Molecular Adsorption. *J. Phys. Chem. C* **2022**, *126*, 12060–12073.

(61) Mino, L.; Cazzaniga, M.; Moriggi, F.; Ceotto, M. Elucidating NOx Surface Chemistry at the Anatase (101) Surface in TiO_2 Nanoparticles. *J. Phys. Chem. C* **2023**, *127*, 437–499.

(62) Micciarelli, M.; Gabas, F.; Conte, R.; Ceotto, M. An Effective Semiclassical Approach to IR Spectroscopy. *J. Chem. Phys.* **2019**, *150*, 184113.

(63) Lanzi, C.; Aieta, C.; Ceotto, M.; Conte, R. A time averaged semiclassical approach to IR spectroscopy. *J. Chem. Phys.* **2024**, *160*, 214107.

(64) Wang, H.; Thoss, M.; Miller, W. H. Forward–backward initial value representation for the calculation of thermal rate constants for reactions in complex molecular systems. *J. Chem. Phys.* **2000**, *112*, 47–55.

(65) Yamamoto, T.; Wang, H.; Miller, W. H. Combining semiclassical time evolution and quantum Boltzmann operator to evaluate reactive flux correlation function for thermal rate constants of complex systems. *J. Chem. Phys.* **2002**, *116*, 7335–7349.

(66) Yamamoto, T.; Miller, W. H. Semiclassical calculation of thermal rate constants in full Cartesian space: The benchmark reaction D+ H2 -> DH+ H. *J. Chem. Phys.* **2003**, *118*, 2135–2152.

(67) Pollak, E.; Martin-Fierro, E. New coherent state representation for the imaginary time propagator with applications to forward-backward semiclassical initial value representations of correlation functions. *J. Chem. Phys.* **2007**, *126*, 164107.

(68) Miller, W. H. Semiclassical limit of quantum mechanical transition state theory for nonseparable systems. *J. Chem. Phys.* **1975**, *62*, 1899–1906.

(69) Wolynes, P. G. Quantum theory of activated events in condensed phases. *Phys. Rev. Lett.* **1981**, *47*, 968.

(70) Liao, J.-L.; Pollak, E. Quantum transition state theory for the collinear H+H_2 reaction. *J. Phys. Chem. A* **2000**, *104*, 1799–1803.

(71) Miller, W. H.; Zhao, Y.; Ceotto, M.; Yang, S. Quantum instanton approximation for thermal rate constants of chemical reactions. *J. Chem. Phys.* **2003**, *119*, 1329–1342.

(72) Ceotto, M.; Miller, W. H. Test of the quantum instanton approximation for thermal rate constants for some collinear reactions. *J. Chem. Phys.* **2004**, *120*, 6356–6362.

(73) Ceotto, M. Vibration-assisted tunneling: a semiclassical instanton approach. *Mol. Phys.* **2012**, *110*, 547–559.

(74) Meisner, J.; Kästner, J. Atom tunneling in chemistry. *Angw. Chem. Intl Ed.* **2016**, *55*, 5400–5413.

(75) Vaillant, C. L.; Thapa, M. J.; Vaníček, J.; Richardson, J. O. Semiclassical analysis of the quantum instanton approximation. *J. Chem. Phys.* **2019**, *151*.

(76) Pollak, E.; Cao, J. Thermal rate of transmission through a barrier: Exact expansion of up to and including terms of order $\hbar^4$. *Phys. Rev. A* **2023**, *107*, 022203.

(77) Miller, W. H. Quantum mechanical transition state theory and a new semiclassical model for reaction rate constants. *J. Chem. Phys.* **1974**, *61*, 1823–1834.

(78) Miller, W. H.; Hernandez, R.; Handy, N. C.; Jayatilaka, D.; Willetts, A. Ab initio calculation of anharmonic constants for a transition state, with application to semiclassical transition state tunneling probabilities. *Chem. Phys. Lett.* **1990**, *172*, 62–68.

(79) Hernandez, R.; Miller, W. H. Semiclassical transition state theory. A new perspective. *Chem. Phys. Lett.* **1993**, *214*, 129–136.

(80) Shan, X.; Burd, T. A.; Clary, D. C. New developments in semiclassical transition-state theory. *J. Phys. Chem. A* **2019**, *123*, 4639–4657.

(81) Miller, W. H. Importance of nonseparability in quantum mechanical transition-state theory. *Acc. Chem. Res.* **1976**, *9*, 306–312.

(82) Wigner, E. P. Über dar Überschreiten von Potentialschwellen bei chemischen Reaktionen. *Zeit. Phys. Chem. B* **1932**, *19*, 203–216.

(83) Nguyen, T. L.; Barker, J. R.; Stanton, J. F. *Adv. Atmosph. Chem.*; World Scientific, 2017; pp 403–492.

(84) Gutzwiller, M. C. Periodic orbits and classical quantization conditions. *J. Math. Phys.* **1971**, *12*, 343–358.

(85) Fröman, N.; Fröman, P. O. JWKB approximation: contributions to the theory. *(No Title)* **1965**,

(86) Miller, W. H. Semi-classical theory for non-separable systems:. Construction of âgoodâ action-angle variables for reaction rate constants. *Farad. Discuss.* **1977**, *62*, 40–46.

(87) Nguyen, T. L.; Stanton, J. F.; Barker, J. R. Ab initio reaction rate constants computed using semiclassical transition-state theory: HO+ H2â H2O+ H and isotopologues. *J. Phys. Chem. A* **2011**, *115*, 5118–5126.

(88) Aieta, C.; Gabas, F.; Ceotto, M. Parallel Implementation of Semiclassical Transition State Theory. *J. Chem. Theory Comput.* **2019**, *15*, 2142–2153.

(89) Aieta, C.; Gabas, F.; Ceotto, M. An Efficient Computational Approach for the Calculation of the Vibrational Density of States. *J. Phys. Chem. A* **2016**, *120*, 4853–4862.

(90) Mandelli, G.; Aieta, C.; Ceotto, M. Heavy atom tunneling in organic reactions at coupled cluster potential accuracy with a parallel implementation of anharmonic constant calculations and semiclassical transition state theory. *J. Chem. Theory Comput.* **2022**, *18*, 623–637.

(91) Wang, F.; Landau, D. P. Efficient, multiple-range random walk algorithm to calculate the density of states. *Phys. Rev. Lett.* **2001**, *86*, 2050.

(92) Wang, F.; Landau, D. Determining the density of states for classical statistical models: A random walk algorithm to produce a flat histogram. *Phys. Rev. E* **2001**, *64*, 056101.

(93) Vogel, T.; Li, Y. W.; Wüst, T.; Landau, D. P. Generic, hierarchical framework for massively parallel Wang-Landau sampling. *Phys. Rev. Lett.* **2013**, *110*, 210603.

(94) Barker, J.; Nguyen, T. L.; Stanton, J. F.; Aieta, C.; Ceotto, M.; Gabas, F.; Kumar, T. J. D.; Li, C. G. L.; Lohr, L. L.; Maranzana, A.; Ortiz, N. F.; Preses, J. M.; Simmie, J. M.; Sonk, J. A.; Stimac, P. J. Multiwell software suite. **2024**,

(95) Barker, J. R. Multiple-Well, multiple-path unimolecular reaction systems. I. MultiWell computer program suite. *Intl J. Chem. Kin.* **2001**, *33*, 232–245.

(96) Brunton, G.; Gray, J. A.; Griller, D.; Barclay, L.; Ingold, K. Kinetic applications of electron paramagnetic resonance spectroscopy. 32. Further studies of quantum-mechanical tunneling in the isomerization of sterically hindered aryl radicals. *J. Am. Chem. Soc.* **1978**, *100*, 4197–4200.

(97) Frisch, M. e.; Trucks, G.; Schlegel, H. B.; Scuseria, G.; Robb, M.; Cheeseman, J.; Scalmani, G.; Barone, V.; Petersson, G.; Nakatsuji, H., et al. Gaussian 16. 2016.

(98) Valiev, M.; Bylaska, E.; Govind, N.; Kowalski, K.; Straatsma, T.; Van Dam, H.; Wang, D.; Nieplocha, J.; Apra, E.; Windus, T.; de Jong, W. NWChem: A comprehensive and scalable open-source solution for large scale molecular simulations. *Comput. Phys. Commun.* **2010**, *181*, 1477–1489.

(99) Barnes, L.; Schindler, B.; Compagnon, I.; Allouche, A.-R. iGVPT2: an interface to computational chemistry packages for anharmonic corrections to vibrational frequencies. *arXiv preprint arXiv:1704.02144* **2017**,

(100) Matthews, D. A.; Cheng, L.; Harding, M. E.; Lipparini, F.; Stopkowicz, S.; Jagau, T.-C.; Szalay, P. G.; Gauss, J.; Stanton, J. F. Coupled-cluster techniques for computational chemistry: The CFOUR program package. *J. Chem. Phys.* **2020**, *152*.

(101) Fornberg, B. Generation of finite difference formulas on arbitrarily spaced grids. *Mathem. Comput.* **1988**, *51*, 699–706.

(102) Carpenter, B. K. Heavy-atom tunneling as the dominant pathway in a solution-phase reaction? Bond shift in antiaromatic annulenes. *J. Am. Chem. Soc.* **1983**, *105*, 1700–1701.

(103) Guner, V.; Khuong, K. S.; Leach, A. G.; Lee, P. S.; Bartberger, M. D.; Houk, K. A standard set of pericyclic reactions of hydrocarbons for the benchmarking of computational methods: the performance of ab initio, density functional, CASSCF, CASPT2, and CBS-QB3 methods for the prediction of activation barriers, reaction energetics, and transition state geometries. *J. Phys. Chem. A* **2003**, *107*, 11445–11459.

(104) Sarkar, S. K.; Solel, E.; Kozuch, S.; Abe, M. Heavy-atom tunneling processes during denitrogenation of 2, 3-diazabicyclo [2.2. 1] hept-2-ene and ring closure of cyclopentane-1, 3-diyl diradical. Stereoselectivity in tunneling and matrix effect. *J. Org. Chem.* **2020**, *85*, 8881–8892.

(105) Castro, C.; Karney, W. L. Heavy-Atom Tunneling in Organic Reactions. *Angw. Chem.* **2020**, *132*, 8431–8442.

(106) Pollak, E.; Cao, J. $\hbar^2$ expansion of the transmission probability through a barrier. *J. Chem. Phys.* **2022**, *157*.

(107) Pollak, E. A personal perspective of the present status and future challenges facing thermal reaction rate theory. *J. Chem. Phys.* **2024**, *160*, 150902.

(108) Althorpe, S. C. On the equivalence of two commonly used forms of semiclassical instanton theory. *J. Chem. Phys.* **2011**, *134*.

(109) Goel, P.; Stanton, J. F. Semiclassical transition state theory based on fourth order vibrational perturbation theory: Model system studies beyond symmetric Eckart barrier. *J. Chem. Phys.* **2018**, *149*.